Effects of Serpin Binding on the Target Proteinase: Global Stabilization, Localized Increased Structural Flexibility, and Conserved Hydrogen Bonding at the Active Site†

Gyula Kaslik,‡ József Kardos,§,‡ Erika Szabó,⊥,‡ László Szilágyi,‡ Péter Závodszky,§ William M. Westler,∥ John L. Markley,∥ and László Gráf *,‡

Department of Biochemistry, Eötvös University, H-1088 Puskin u. 3, Budapest, Hungary, Institute of Enzymology, Biological Research Center, Hungarian Academy of Sciences, H-1119, Karolina u. 29, Budapest, Hungary, Agricultural Biotechnology Center, P.O.B. 411, H-2100 Godollo, Hungary, and Department of Biochemistry and National Magnetic Resonance Facility at Madison, University of Wisconsin−Madison, Madison, Wisconsin 53706

Received December 2, 1996; Revised Manuscript Received February 10, 1997⊗

ABSTRACT: The binding of human α_1-proteinase inhibitor to rat trypsin was shown by NMR spectroscopy to raise the pK_a' of His^{57} in the active site but not to disrupt the hydrogen bond between His^{57} and Asp^{102}. Similar NMR results were observed for the Asp^{189} to serine mutant of rat trypsin, which is much more stable than wild-type trypsin against autoproteolysis as the result of mutation of the residue at the base of the specificity pocket. This mutant was used in further studies aimed at determining the extent of the conformational transition in trypsin that accompanies serpin binding and leads to disruption of the catalytic activity of the proteinase such that the inhibitor complex is trapped at the acyl enzyme intermediate stage. The stability of rat trypsin toward thermal denaturation was found to be lower in the free enzyme than in the complex with α_1-proteinase inhibitor. This suggests that the complex contains extensive protein−protein interactions that stabilize overall folding. On the other hand, previous investigations have shown that the proteinase in serpin−proteinase complexes becomes more susceptible to limited proteolysis, suggesting that the conformational change that accompanies binding leads to the exposure of susceptible loops in the enzyme. The existence of this type of conformational change upon complex formation has been confirmed here by investigation of the rate of cleavage of disulfide linkages by added dithiothreitol. This study revealed that, despite the increased stability of trypsin in the complex, one or more of its disulfide bridges becomes much more easily reduced. We suggest that the process of complex formation with α_1-proteinase inhibitor converts trypsin D189S into an inactive, loose structure, which serves as a "conformational trap" of the enzyme that prevents catalytic deacylation. It is also proposed that plastic region(s) of the activation domain of trypsin may play a crucial role in this inhibitor-induced structural rearrangement.

The serpin superfamily of serine proteinase inhibitors comprises a group of structurally related proteins that control a variety of physiological processes (coagulation, fibrinolysis, complement activation, etc.). Target proteinases interact at a reactive site on the surface of the serpin located within an exposed mobile reactive site loop (RSL)[1] structure. Structures of both intact and modified (reactive site cleaved) serpins have been determined by X-ray crystallography. These studies have shown that the RSL in intact serpins is variable: it can adopt a conformation that resembles the canonical loop conformation found in all other families of protein serine proteinase inhibitors (Elliott et al., 1996), or the RSL can form a distorted helix which is held well away from the body of the serpin by two extended strands with no stabilizing intramolecular contacts (Wei et al., 1994; Song et al., 1995). In the proteolytically modified serpins, the P1 and P1′ [2] residues are separated by 70 Å and are located on opposite sides of the molecule as a consequence of insertion

† Work in Budapest was supported by a grant of the Hungarian Academy of Sciences to L.G., by Grant OTKA T 013303 to L.S., by Grants OTKA T 017478 and OTKA T 5206 to P.Z., by a "For National Science" Grant of Hungarian Credit Bank to G.K., and by a Peregrinatio II Foundation (ELTE) grant to G.K. Work in Madison was supported by NIH Grant GM35976. NMR spectroscopy was carried out at the National Magnetic Resonance Facility at Madison which is funded by NIH Grant RR02301; equipment in the Facility was purchased with funds from the University of Wisconsin, the NSF Biological Instrumentation Program (Grant DMB-8415048), the National Biomedical Research Technology Program (Grant RR02301), NIH Shared Instrumentation Program (Grant RR02781), and the U.S. Department of Agriculture.

* To whom correspondence should be addressed.
‡ Eötvös University.
§ Hungarian Academy of Sciences.
⊥ Agricultural Biotechnology Center.
∥ University of Wisconsin−Madison.

⊗ Abstract published in *Advance ACS Abstracts,* April 1, 1997.

[1] Abbreviations: α_1-PI, human α_1-proteinase inhibitor; α_1-PI*, modified human α_1-proteinase inhibitor; AMC, 7-amino-4-methylcoumarin; ANS, 8-anilinonaphthalene-1-sulfonate; ATIII, antithrombin III; BPTI, bovine pancreatic trypsin inhibitor (Kunitz); CD, circular dichroism; D189S, mutant in which aspartate-189 (residue at the base of the specificity pocket in trypsin) is replaced by serine (corresponding residue to chymotrypsin); DSC, differential scanning calorimetry; DTT, dithiothreitol; FPLC, fast protein liquid chromatography; GdnHCl, guanidinium chloride; HNE, human neutrophil elastase; PAGE, polyacrylamide gel electrophoresis; RSL, reactive site loop; SDS, sodium dodecyl sulfate; STI, soybean trypsin inhibitor (Kunitz); Suc, succinyl; TCA, trichloroacetic acid; T_m, the temperature of maximal heat capacity; TPCK, *N*-tosyl-L-phenylalanine chloromethyl ketone; TUG, transverse urea gradient; Tris, tris(hydroxymethyl)aminomethane.

[2] The nomenclature of Schechter and Berger (1967) is used to define residues in the reactive site of inhibitors. The residue on the N-terminal side of the scissile bond is termed P_1.

S0006-2960(96)02931-5 CCC: $14.00

of the cleaved RSL as strand S4A into an antiparallel six-stranded β-sheet (Löbermann et al., 1984; Baumann et al., 1991, 1992; Mourey et al., 1993; Aertgeerts et al., 1995). This loop insertion leads to a dramatic increase in structural stability, as indicated by CD and NMR studies (Gettins & Harten, 1988; Bruch et al., 1988), heat denaturation (Carell & Owen, 1985; Carell et al., 1991), and $^1H-^2H$ exchange within the polypeptide backbone as indicated by results from FT-IR and NMR spectroscopy (Haris et al., 1990).

No structure is available for a serpin−proteinase complex, and the mechanism by which serpins inhibit their target proteinases is not known in detail. A body of work suggests that proteinase interaction with serpins is reversible and does not produce RSL cleavage (Shieh et al., 1989; Matheson et al., 1991; Enghild et al., 1994; Christensen et al., 1995). Recent studies, however, have provided evidence that the RSL is cleaved in the serpin−proteinase complex and that the complex consists of an unusually stable acyl-enzyme intermediate (Shore et al., 1995; Kaslik et al., 1995; Lawrence et al., 1995; Wilczynska et al., 1995; Engh et al., 1995).

The results of thermal and chemical denaturation experiments indicate that both components are more stable in the proteinase−serpin complex than in separated forms (Atha et al., 1984; Lennick et al., 1985; Mast et al., 1991; Komiyama et al., 1994; Enghild et al., 1994) and that in these experiments the behavior of serpins in the complex is similar to that of the cleaved, RSL-inserted form of the inhibitor [see also Shore et al. (1995), Lawrence et al. (1995), Plotnick et al. (1996), Mast et al. (1991), Björk et al. (1993), Olson et al. (1995), and Debrock and Declerck (1995)]. In contrast to these results from thermal and chemical denaturation, we have recently reported that the D189S mutant of rat trypsin, when complexed with human α_1-proteinase inhibitor (α_1-PI), becomes more susceptible to limited proteolysis (Kaslik et al., 1995); this indicates that at least the first cleavage site is more accessible to proteinase in the complex than in uncomplexed trypsin. Trypsin D189S was used in these studies in preference to wild-type rat trypsin because its autolysis is not significant (Kaslik et al., 1995) as the result of lowered catalytic activity (Gráf et al., 1988). The more recent report by Stavridi et al. (1996) that α-chymotrypsin when complexed with α_1-antichymotrypsin also shows increased susceptibility to proteolysis suggests that this may be a general property of serpin−proteinase complexes. The existence of a structural change in the proteinase upon complex formation was suggested by earlier fluorescence spectroscopic results (Hervé & Ghélis, 1991). Furthermore, it has been concluded from a recent NMR investigation that the hydrogen bond between His^{57} and Asp^{102} of the catalytic triad is disrupted in the complex (Plotnick et al., 1996).

The aims of the present study were to investigate these apparently contradictory conclusions about the state of the proteinase in serpin−proteinase complexes: greater stability on the one hand and greater susceptibility to proteolysis and disruption of the active site on the other. We used several approaches to compare the structure and properties of rat trypsin with its complex with human α_1-PI. These included investigations of the state of His^{57} by NMR spectroscopy, studies of protein stability against urea denaturation, as followed by both tryptophan fluorescence and transverse urea gradient gels, and against thermal unfolding, as monitored by both near- and far-UV circular dichroism (CD) spectroscopy and differential scanning calorimetry (DSC), studies of the rate of disulfide bridge reduction by dithiothreitol (DTT), and investigations of hydrophobic binding propensity as shown by perturbation of the fluorescence spectrum of 8-anilinonaphthalene-1-sulfonate (ANS). Our results confirm that the proteinase undergoes a major structural rearrangement upon complex formation with serpin but reveal that this rearrangement does not disrupt hydrogen bonding of the catalytic histidine which titrates in the complex but with a pK_a' about one pH unit higher than in free trypsin. Protein−protein interactions in the complex lead to thermal stabilization of trypsin, but the structure is distorted in a way that makes one or more disulfide bridges accessible to reduction and hydrophobic regions accessible to ANS binding. These changes likely are part of the mechanism that leads to deactivation of the catalytic apparatus and consequently to the stability of the acyl linkage between the enzyme and inhibitor.

EXPERIMENTAL PROCEDURES

Materials. The tetrapeptide substrate Suc-Ala-Ala-Pro-Tyr-AMC, with fluorogenic leaving group 7-amino-4-methylcoumarin (AMC), was synthesized as described previously (Gráf et al., 1988). Bovine pancreatic trypsin inactivated by TPCK to remove chymotryptic activity was purchased from Sigma (St. Louis, MO). The D189S mutant of rat trypsinogen was produced in an *Escherichia coli* expression−secretion system, purified to homogeneity, and activated by enterokinase, as described previously (Gráf et al., 1988; Corey & Craik, 1992). Human α_1-PI was purchased from Serva (Heidelberg, Germany) and purified to homogeneity (Kaslik et al., 1995). Preparation and isolation of the rat trypsin D189S−α_1-PI complex was carried out according to the method described by Kaslik et al. (1995). The purified proteins were stored at −20 °C.

Preparation of Modified α_1-PI. α_1-PI was incubated with bovine TPCK trypsin in 1:1 molar ratio in 0.1 M Tris-HCl buffer, pH 8.5, and 0.5 M hydroxylamine for 8 h at 37 °C [see Moroi and Yamasaki (1974), Owen (1975), Johnson and Travis (1976), Cohen et al. (1978), Wiman and Collen (1979), Nilsson et al. (1983), and Lindahl et al. (1990)]. The modified α_1-PI was separated from bovine trypsin on a Mono Q ion exchange column (Pharmacia FPLC system, Uppsala, Sweden); the elution buffer was a 10 mM sodium citrate-phosphate with a linear pH gradient from pH 7.0 to 5.0 and a linear salt gradient from 0.0 to 0.2 M NaCl. The separation was followed by SDS−PAGE. The purified α_1-PI* was stored at −20 °C.

Enzyme Assays. Complex formation between trypsin D189S and α_1-PI was monitored by loss of proteolytic activity. The substrate was 10 μM Suc-Ala-Ala-Pro-Tyr-AMC, which has a fluorogenic leaving group (AMC) and which was dissolved in sodium acetate buffer, pH 5.4. Assays were performed at 20 °C. We used eq 1 in determining the second-order rate constant k for the reaction, because the initial concentrations of components were equal and the substrate concentration was much less than the K_m of trypsin D189S (Gráf et al., 1988).

$$k = [E]/t[E]_o([E]_o - [E]) \quad (1)$$

where the equal initial concentrations of the enzyme and the inhibitor are represented by $[E]_o$ ($[E]_o = [I]_o = 1$ μM) and

where the equal concentrations of free enzyme and inhibitor at time *t* are represented by [E]. The concentration of free enzyme [E] at time *t* was calculated from

$$[E] = [E]_o T/T_o \quad (2)$$

where T_o was the slope of the plot (the change in fluorescence due to the release of AMC *versus* the change in time) for the enzyme in the absence of α_1-PI, and *T* was the slope at time *t* following the addition of α_1-PI. Excitation/emission wavelengths were 366/450 nm, and all measurements were carried out with a SPEX FluoroMax spectrofluorometer (Jobin-Yvon, Longjumeau Cedex, France). The effect of 100 μM ANS on the activity of trypsin D189S was measured in 10 mM sodium acetate buffer, pH 5.4, at 20 °C and at substrate concentrations much less than K_m for the mutant trypsin.

NMR Spectroscopy. Solutions used for NMR spectroscopy contained approximately 1 mM trypsin and 0.4 mM complex dissolved in 90:10 ^1H_2O:^2H_2O. The pH was measured with a small combination glass electrode, and pH adjustments were made by KOH or HCl. ^{1}H NMR data were collected on a 500 MHz Bruker DMX spectrometer (Billerica, MA) at the National Magnetic Resonance Facility at Madison. A 1−1 pulse sequence (Hore, 1983) was used for data acquisition. Spectra were processed with the FELIX software package (Biosym, San Diego, CA) on Silicon Graphics (Montain View, CA) workstations.

Transverse Urea Gradient (TUG) Polyacrylamide Gel Electrophoresis. TUG gels were prepared as described by Creighton (1979). A peristaltic pump was used to make slab gels (13 cm × 12 cm × 0.1 cm) containing a 0−8 M urea gradient perpendicular to the direction of electrophoresis and a gradient of 15−11% acrylamide to the opposite direction. Samples containing approximately 100 μg of protein in a total volume of 150−200 μL were layered onto the top of the gel. Electrophoresis was performed in 50 mM Tris-HCl buffer, pH 8.0, at room temperature with a constant current 20 mA/gel. The gels were stained with Coomassie Brilliant Blue. The low isoelectric point of rat trypsin allowed it to enter the gel under the conditions used.

Unfolding in Urea. Samples of α_1-PI*, trypsin D189S, and the trypsin D189S−α_1-PI complex were dissolved in solutions of 10 mM sodium acetate buffer, pH 5.4, containing various concentrations of urea (0−9 M). The samples were incubated for 8 h at 20 °C before the fluoresence was measured. Protein concentrations were adjusted such that $A_{280} \leq 0.05$. Denaturation transition curves were obtained from the wavelength of the tryptophan fluorescence maximum determined with the SPEX FluoroMax spectrofluorimeter. The excitation wavelength was 295 nm.

Circular Dichroism Spectroscopy. CD measurements were carried out on a Jasco J-720 spectropolarimeter (Tokyo, Japan) equipped with a Neslab RTE-100 computer-controlled thermostat over the temperature range 25−95 °C. Samples were placed in cylindrical, water-jacketed quartz cells. For recording far-UV spectra, cells of 0.1 and 0.01 cm were used, and the protein concentrations were 0.2−1.0 mg/mL. When measuring near-UV spectra, 1.0 cm cells were used, and the protein concentrations were 0.5 mg/mL. All samples were dialyzed against 10 mM sodium acetate buffer, pH 5.4. For heat denaturation studies, cells with 0.1 cm pathlength were used, and the protein concentration was 0.5−1.0 mg/mL. Unfolding of secondary structure was monitored at 217 nm in the far-UV region, and changes in the environment of side chains, reflecting changes in the tertiary structure of the protein molecules were followed at 282 nm in the near-UV region. The heating rate was 50 °C/h.

Differential Scanning Calorimetry. Calorimetric measurements were performed on a DASM-4 instrument (Poushchino, Russia). Denaturation curves were recorded between 10 and 125 °C at a pressure of 2.5 atm using a scan rate of 1 °C/min. Samples were dialyzed extensively against 10 mM sodium acetate buffer, pH 5.4, and the dialysis buffer was used as a reference. Protein concentrations were set to 3 mg/mL for the trypsin D189S−α_1-PI complex and 1 mg/mL for trypsin D189S, α_1-PI, and α_1-PI*. Heat capacities were calculated as described by Privalov (1979).

ANS Binding Experiments. Separate samples of 1 μM α_1-PI, 1 μM α_1-PI*, 1 μM trypsin D189S, equimolar (1 μM:1 μM) trypsin D189S plus α_1-PI, and equimolar (1 μM:1 μM) trypsin D189S plus α_1-PI* were made up at 20 °C in 10 mM sodium acetate buffer, pH 5.4, containing 100 μM ANS. Immediately after the solution of trypsin D189S plus α_1-PI was made up, formation of the trypsin D189S−α_1-PI complex was followed at 20 °C in this solvent mixture with a SPEX FluoroMax spectrofluorimeter. Excitation/emission wavelengths were 370/460 nm. The second-order rate constant for complex formation *k* was determined from eq 1.

Limited Reduction Experiments. Separate samples of 20 μM trypsin D189S and its α_1-PI complex were incubated with 0, 1, and 10 mM dithiothreitol (DTT) in 0.1 M Tris-HCl buffer, pH 8.5, at room temperature for 40 min. The reduction reaction was terminated by adding iodoacetamide at a concentration 4 times that of DTT and incubating for 20 min. To achieve complex dissociation, hydroxylamine at a final concentration of 0.5 M was added to each sample, and the samples were treated at 37 °C for 12 h [see Moroi and Yamasaki (1974), Owen (1975), Johnson and Travis (1976), Cohen et al. (1978), Wiman and Collen (1979), Nilsson et al. (1983), and Lindahl et al. (1990)]. At the end of this period, 20% (v/v) trichloroacetic acid (TCA) was added, samples were incubated for 20 min at 0 °C, and the precipitated protein was isolated by centrifugation at 17000*g* for 10 min. The supernatant from each sample was discarded, and the precipitated protein was dissolved in a SDS−PAGE sample buffer without 2-mercaptoethanol. The control sample was reduced by adding excess amount of 2-mercaptoethanol. All samples were boiled for 3 min and analyzed by SDS−PAGE (Laemmli, 1970) on 15% (w/v) polyacrylamide gels. The identity of the band representing the completely reduced form of trypsin D189S was confirmed by immunoblotting.

RESULTS

NMR Spectroscopy. The goals of the NMR experiments were to investigate the titration properties of His^{57} in the free wild-type and mutant trypsins and in their α_1-PI complexes. Figure 1 shows the far lowfield region of the ^{1}H NMR spectra acquired at different pH values of (A) rat trypsin, (B) the rat trypsin−α_1-PI complex, (C) D189S rat trypsin, and (D) the D189S rat trypsin−α_1-PI complex. At pH 3, both wild-type and D189S trypsin showed a peak at about 17.4 ppm of the kind assigned to the proton in the hydrogen bond between positively-charged His^{57} and nega-

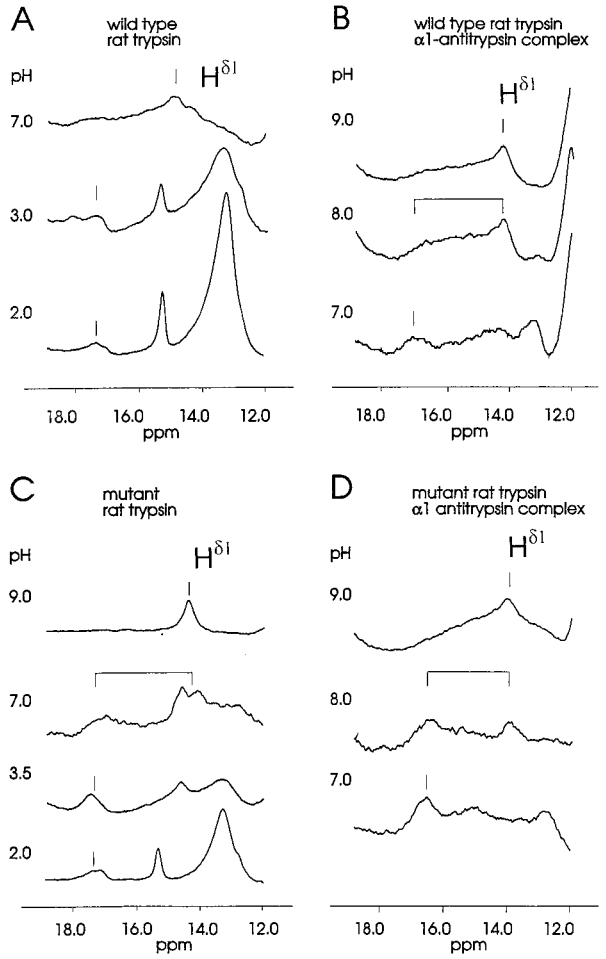

FIGURE 1: Histidine ring amide region of 500 MHz ^{1}H NMR spectra of (A) wild-type rat trypsin, (B) the complex between wild-type rat trypsin and human α_1-proteinase inhibitor, (C) rat trypsin D189S, and (D) the complex between rat trypsin D189S and human α_1-proteinase inhibitor. The protein samples were dissolved in 90%:10% H_2O:^2H_2O. Glass electrode pH meter readings for individual spectra are shown in the figure. The position of the signals are attributed to the proton hydrogen bonded between Asp[102] and His[57] are indicated. Two signals are observed at pH values near the pK of His[57] because its protonation−deprotonation is slow on the chemical shift time scale: the signal with the larger chemical shift arises from protonated His[57], and the signal with the smaller chemical shift arises from neutral His[57].

tively-charged Asp[102] at the active site of serine proteinases (Robillard & Shulman, 1974; Markley, 1979). As the pH was raised, the intensity of this peak decreased, and a peak grew in at 14.5−14.7 ppm. The areas of the two peaks became equivalent at a pH value near 7.0. Similar peaks were seen in spectra of the two α_1-PI complexes, but the chemical shifts were about 17.0 ppm for the low-pH form and about 14.3 ppm for the high-pH form, and the intensities of the two peaks became equivalent near pH 8.0. All samples studied at pH values below 4 exhibited a sharp peak near 15.5 ppm whose intensity increased as the pH was lowered.

Transverse Urea Gradient Polyacrylamide Gel Electrophoresis. TUG gels were chosen as a technique to further investigate the nature of structural differences between trypsin alone and complexed with α_1-PI. The urea concentration at which an unfolding transition occurs can be visualized by this method, because the unfolded protein occupies a larger hydrodynamic volume than the folded protein and thus migrates more slowly (Goldenberg, 1989).

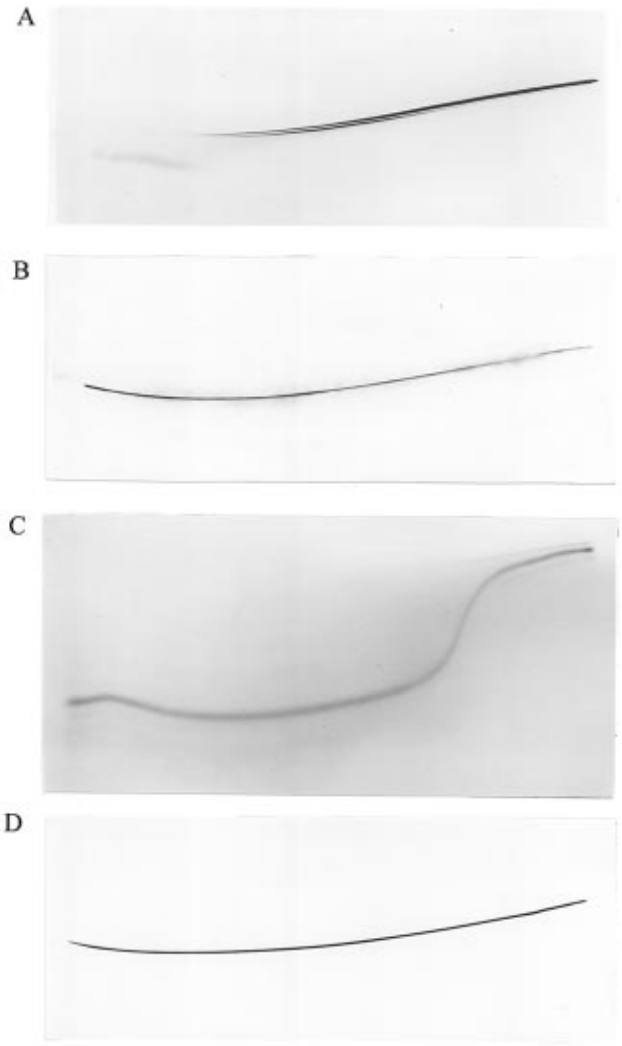

FIGURE 2: Visualization by transverse urea polyacrylamide gel electrophoresis (TUG−PAGE) of the conformation stabilities of: (A) human α_1-proteinase inhibitor (α_1-PI), (B) cleaved α_1-proteinase inhibitor (α_1-PI*), (C) rat trypsin D189S, and (D) the complex between trypsin D189S and α_1-proteinase inhibitor. For each gel, the direction of migration was from top to bottom, and the urea gradient (0−8 M) was from left to right. Gels were stained with Coomassie Brilliant Blue.

TUG gels of α_1-PI, α_1-PI*, rat trypsin D189S, and the rat trypsin D189S−α_1-PI complex are shown in Figure 2. Whereas a clear unfolding transition was observed for α_1-PI at low urea concentration (1−2 M) (Figure 2A), no unfolding transition was detected for α_1-PI* up to 8 M urea (Figure 2B). Similarly, whereas rat trypsin D189S showed an unfolding transition at about 6 M urea (Figure 2C), the rat trypsin D189S−α_1-PI complex showed no transition (Figure 2D).

Unfolding in Urea. Urea-induced unfolding was monitored from the shift in the emission maximum of the intrinsic fluorescence of the proteins (Figure 3). In this experiment, α_1-PI showed two transitions, one near 2 M urea (which may correspond to the transition in hydrodynamic volume detected by TUG) and one near 5.2 M urea (which apparently does not affect the hydrodynamic volume) (Figure 3A), whereas α_1-PI* exhibited no transition (in agreement with the TUG results) (Figure 3B). By contrast, both rat trypsin D189S and its complex with α_1-PI showed transitions near 6 M urea. Trypsin D189S exhibited a single, steep transition centered at 6.2 M urea (Figure 3C) similar to its TUG gel behavior.

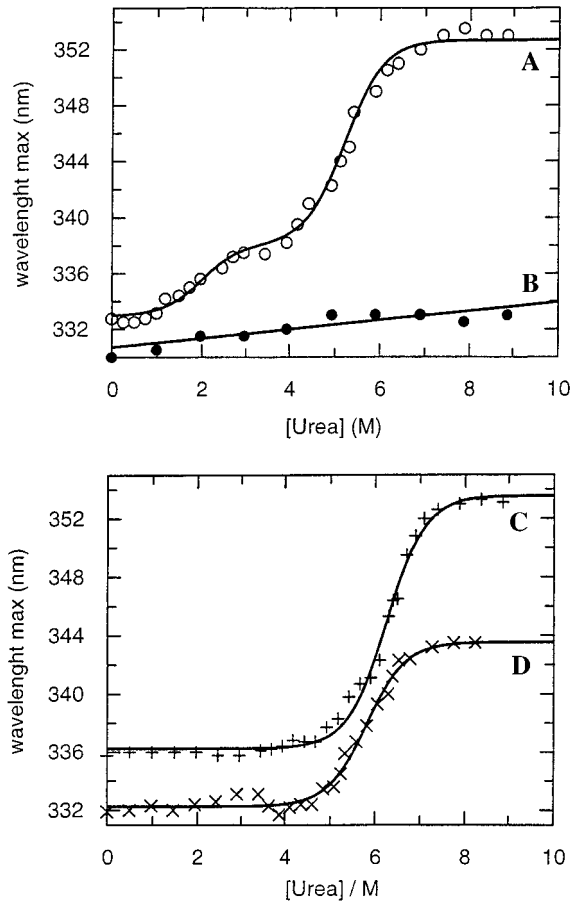

FIGURE 3: Comparison of the urea-induced unfolding transition of (A) human α_1-proteinase inhibitor (α_1-PI), (B) cleaved α_1-proteinase inhibitor (α_1-PI*), (C) rat trypsin D189S, and (D) the complex between trypsin D189S and α_1-proteinase inhibitor. In the top panel, α_1-PI (○, A), α_1-PI* (●, B); in the bottom panel, trypsin D189S (+, C) and trypsin D189S−α_1-PI complex (×, D). The transitions were monitored from changes in the wavelength of the intrinsic Trp fluorescence at 20 °C; excitation was at 295 nm. Aliquots of concentrated protein were mixed with urea to make up samples with urea concentrations between 0 and 9 M urea. All solutions were in 10 mM sodium-acetate buffer, pH 5.4. After mixing, all samples were incubated for 8 h at 20 °C prior to recording spectra.

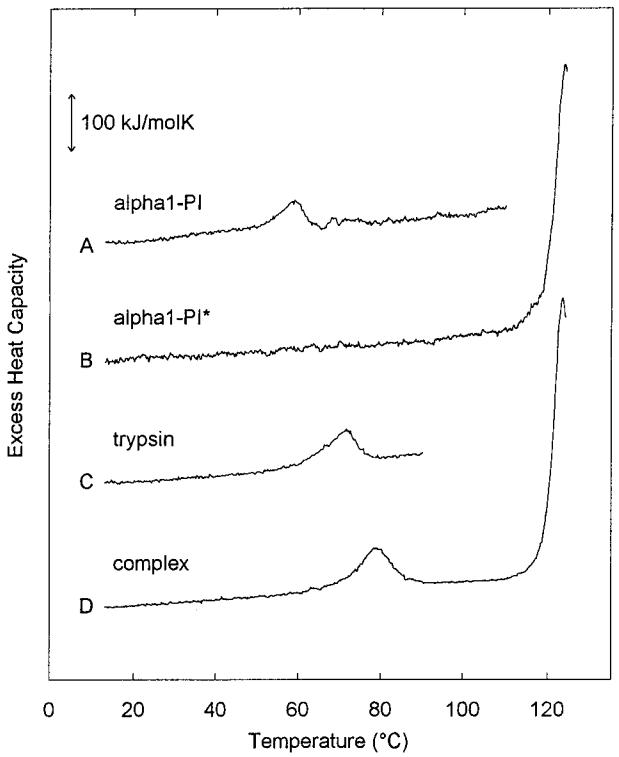

FIGURE 4: Differential scanning calorimetric curves of (A) human α_1-proteinase inhibitor (α_1-PI), (B) cleaved α_1-proteinase inhibitor (α_1-PI*), (C) rat trypsin D189S, and (D) the complex between trypsin D189S and α_1-proteinase inhibitor. Components of the complex can be identified in the thermal scan. The thermal stability of trypsin in the complex is increased significantly (curve D, first peak at 79 °C). The melting profile of complexed α_1-PI (curve D, peak at 123.5 °C) is similar to, if not identical with, that of α_1-PI* (curve B, peak at 124 °C).

However, the trypsin D189S−α_1-PI complex exhibited a shallower, less steep transition step centered at 5.8 M urea (Figure 3D) which was not detected by TUG. For this reason, and because the tryptophan fluorescence emission plateaus at 344 nm, between the values for the folded (332 nm) and unfolded protein (353 nm estimated as the average of the emission maximum for unfolded trypsin D189S and α_1-PI), the urea-induced conformational change appears to be local.

Differential Scanning Calorimetry. Native α_1-PI was found to undergo a temperature-induced transition with a melting temperature of $T_m = 59$ °C (Figure 4A), and no other transition was detected at temperature up to 125 °C. The cleaved form (α_1-PI*), however, showed a sharp, highly cooperative unfolding transition at the much higher temperature value of $T_m = 124$ °C, near the temperature limit of the instrument (Figure 4B). The heat absorption curve of rat trypsin D189S exhibited a cooperative transition with a melting temperature of 72 °C (Figure 4C). In the heat capacity curve of rat trypsin D189S complexed with α_1-PI, the unfolding transitions of the individual components can be identified unambiguously (Figure 4D). The heat absorption peak of α_1-PI in the complex ($T_m = 123.5$ °C) is very similar to the peak of the cleaved α_1-PI*, both in its sharpness and amplitude; the values of the melting temperatures are within 0.5 °C. Rat trypsin D189S in the complex showed a cooperative melting transition with $T_m = 79$ °C (Figure 4D), which is 7 °C higher than the unfolding temperature of native trypsin (Figure 4C).

Circular Dichroism Spectroscopy. The temperature dependence of the mean residue ellipticity for the rat trypsin D189S−α_1-PI complex and an equimolar mixture of rat trypsin D189S and α_1-PI* are compared at 217 nm in the far-UV (Figure 5A) and at 282 nm in the near UV (Figure 5B). The mixture of trypsin D189S and α_1-PI* showed transitions around 72 °C at both wavelengths, close to what is observed by calorimetry; the near-UV scan exhibited a complex transition ($T_m = 73$ °C) complicated by precipitation. Surprisingly, the trypsin−α_1-PI complex did not exhibit a well-defined, cooperative, thermally induced transition in the far-UV, despite the clear transition observed by calorimetry and near-UV circular dichroism temperature dependent experiments. This observation indicates that the secondary structure of trypsin in the complex is not affected significantly during this melting transition. The thermally induced transition in the near UV is close to that observed by calorimetry ($T_m = 78.5$ °C).

Fluorescence Studies of ANS Binding. The fluorescence intensity of ANS is known to increase when the probe binds to solvent-accessible clusters of nonpolar groups in a protein

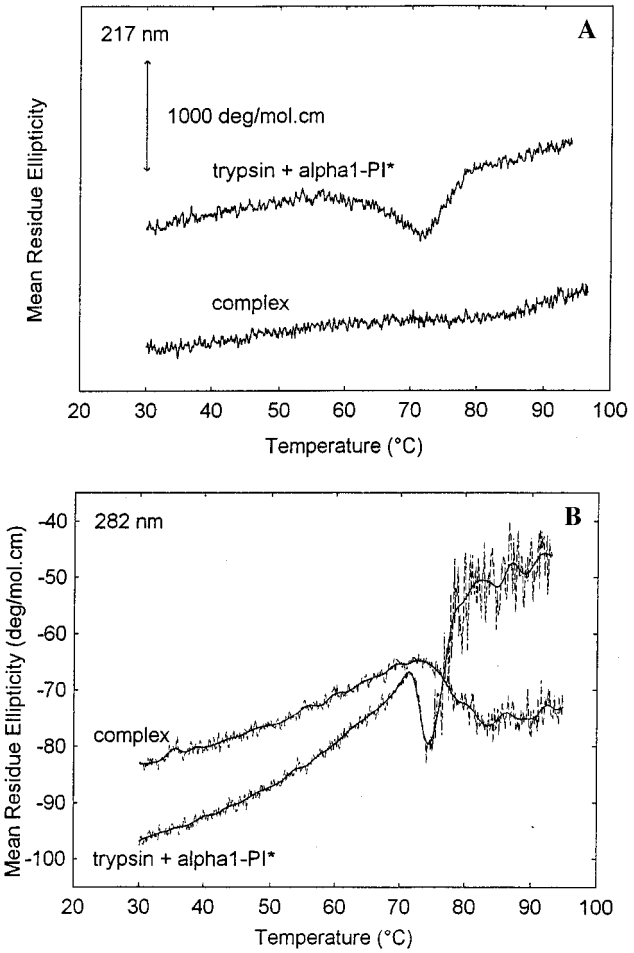

FIGURE 5: Comparison of temperature dependent circular dichroism properties of the complex between rat trypsin D189S and human α_1-proteinase inhibitor (α_1-PI) with those of an equimolar mixture of trypsin D189S and cleaved α_1-proteinase inhibitor (α_1-PI*) as monitored at (A) 217 nm in the far-UV and (B) 282 nm in the near-UV. When monitored at 217 nm, the trypsin D189S−α_1-PI complex shows no significant changes in the secondary structure while the trypsin D189S/α_1-PI* mixture shows a temperature induced transition around 72 °C. When monitored at 282 nm, both the complex and the mixture show clear transitions at temperature values consistent with the results of the calorimetric measurements. The mixture shows evidence of precipitation of trypsin during the transition.

(Stryer, 1965). When rat trypsin D189S and α_1-PI were mixed in the presence of ANS, the fluorescence was found to increase with time. Figure 6 shows experimental data (heavy line) that have been fitted to a second-order rate equation with $k = 6.6 \times 10^3$ M^{-1} s^{-1} (light curve). This association rate is somewhat slower than that determined from the change in the rate of hydrolysis of the substrate Suc-Ala-Ala-Pro-Tyr-AMC by trypsin D189S following the addition of equimolar α_1-PI ($k = 2.3 \times 10^4$ M^{-1} s^{-1}). We found, however, that the catalytic efficiency (k_{cat}/K_m) of trypsin D189S in the presence of 100 μM ANS is only 51% of that measured in the absence of ANS. When this difference was taken into account, the rate of complex formation determined from the enzyme assay coincided with that determined from the time dependence of the fluorescence.

Table 1 summarizes the fluorescence intensities determined for solutions of trypsin D189S, α_1-PI, α_1-PI*, and the equimolar mixtures of trypsin D189S:α_1-PI* and trypsin D189S:α_1-PI, all in the presence of 100 μM ANS. Immediately after mixing, the fluorescence intensities of the equimolar mixtures were found to be similar to the sum of the fluorescence intensities of the components. This suggests that there is no significant interaction between either the proteinase and the modified inhibitor or the proteinase and the active inhibitor as $t \rightarrow 0$. However, formation of the trypsin D189S−α_1-PI complex is accompanied by a remarkable increase in fluorescence intensity. Because other lines of evidence suggest that the structure of the inhibitor in the complex is more like that of α_1-PI* than of α_1-PI (Figure 4B,D and see Shore et al. (1995), Lawrence et al. (1995), Plotnick et al. (1996), and Mast et al. (1991); Björk et al., 1993; Olson et al., 1995; Debrock & Declerck, 1995], and since the enhancement of ANS fluorescence is much lower for α_1-PI* than for α_1-PI (Table 1), it seems likely that the conformational change leading to enhanced ANS binding occurs primarily in the proteinase.

Table 1: ANS Fluorescence Intensity[a]

	fluorescence intensity × 10^5 cps
trypsin D189S	0.98
α_1-proteinase inhibitor (α_1-PI)	6.00
cleaved α_1-proteinase inhibitor (α_1-PI*)	0.42
trypsin D189S + α_1-PI*	1.60
trypsin D189S + α_1-PI	
$t \rightarrow 0$	7.10
$t \rightarrow \infty$	10.2

[a] ANS fluorescence intensity of 1 μM rat trypsin D189S, 1 μM human α_1-proteinase inhibitor (α_1-PI), 1 μM cleaved human α_1-proteinase inhibitor (α_1-PI*), the equimolar (1:1 μM) mixture of trypsin D189S and α_1-PI*, and the equimolar (1:1 μM) mixture of trypsin D189S and α_1-PI at $t \rightarrow 0$ and at $t \rightarrow \infty$. All spectra were recorded with a SPEX FluoroMax spectrofluorimeter at 20 °C in 10 mM sodium acetate buffer, pH 5.4, containing 100 μM ANS. Excitation/emission wavelengths were 370/460 nm.

Rates of Disulfide Bond Reduction. Because rat trypsin contains six disulfide bridges while α_1-PI contains none, studies of changes in the rate of reduction of disulfide bridges upon complex formation provide information selectively about the structure of the proteinase. Trypsin D189S and its complex with α_1-PI were incubated with different concentrations of DTT (0, 1, and 10 mM), and then hydroxylamine treatment was used to dissociate the complex [see Moroi and Yamasaki (1974), Owen (1975), Johnson and Travis (1976), Cohen et al. (1978), Wiman and Collen (1979), Nilsson et al. (1983), and Lindahl et al. (1990)]. As shown in Figure 7, this treatment converts the complex (panel A, lane 1) into two lower molecular weight proteins (Figure 7A, lane 2) corresponding to α_1-PI* (higher M_r) and trypsin D189S (lower M_r). Upon reduction by 1 mM (Figure 7A, lane 3) or 10 mM (Figure 7A, lane 4) DTT, trypsin migrates more slowly because it occupies a larger hydrodynamic volume. Complexed trypsin D189S was found to be much more susceptible to reduction than trypsin D189S is in its uncomplexed form (Figure 7B, lanes 1−4). Trypsin D189S released from the complex incubated with 1 mM DTT appeared to be fully reduced, whereas only two or three disulfide bridges were reduced in uncomplexed trypsin D189S even at 10 mM DTT (Figure 7). The rightmost lane in each panel shows SDS−PAGE of samples reduced completely by treatment with excess 2-mercaptoethanol (Figure 7A,B, lane 5).

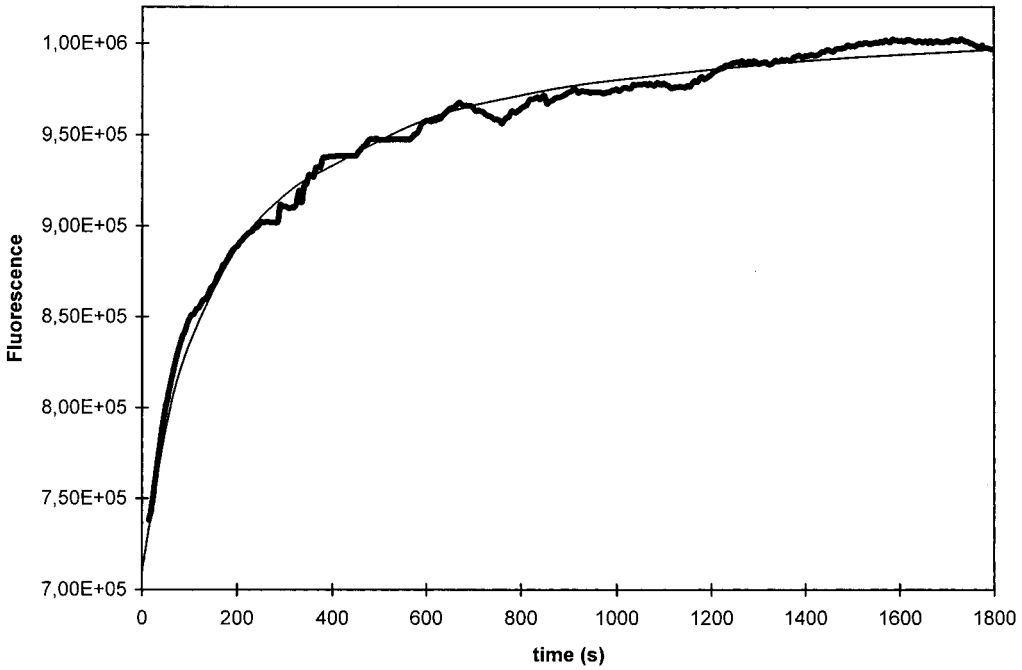

FIGURE 6: Increase in ANS fluorescence accompanying formation of the complex between rat trypsin D189S and α_1-proteinase inhibitor (α_1-PI). Sufficient α_1-PI was added to 10 mM sodium-acetate buffer, pH 5.4, containing 1 μM trypsin D189S and 100 μM ANS in a thermostatted cuvette at 20 °C to achieve a 1:1 inhibitor−proteinase complex. The experimental increase in ANS fluorescence that accompanies complex formation is shown along with a theoretical curve for the first-order process (eq 1). Excitation/emission wavelengths were 370/460 nm.

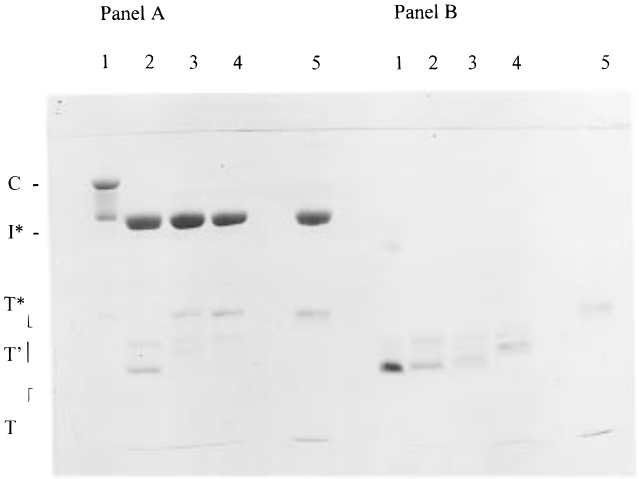

FIGURE 7: Non-reducing SDS−PAGE analysis of disulfide bond reduction (panel A) in 20 μM rat trypsin D189S−α_1-PI complex and (panel B) 20 μM trypsin D189S. Aliquots of trypsin were treated with 0, 1, and 10 mM DTT, respectively, in 0.1 M Tris−HCl buffer, pH 8.5, at room temperature for 40 min. The reduction reaction was terminated by adding iodoacetamide at a concentration 4 times that of DTT and incubating for 20 min. Then each sample (except for the controls; see below) was incubated for 12 h at 37 °C with 0.5 M hydroxylamine, which promotes dissociation of the complex. The protein was next precipitated with 20% (v/v) TCA. In both panels, lane 1 is the control (starting protein without hydroxylamine treatment), lanes 2, 3, and 4 are the precipitated protein samples dissolved in non-reducing SDS−PAGE sample buffer; and lane 5 fully reduced protein (half of the sample incubated with 0 mM DTT dissolved in SDS−PAGE sample buffer containing excess amount of 2-mercaptoethanol). C, trypsin D189S−α_1-PI complex; I*, α_1-PI*; T*, fully reduced trypsin D189S; T′, partially reduced trypsin D189S; T, unreduced trypsin D189S.

DISCUSSION

NMR Evidence for a Change in the Properties of Trypsin upon Complex Formation. The chemical shifts and pH dependence of the low-field N−H peaks observed in spectra of wild-type rat trypsin and rat trypsin D189S are characteristic for the proton in the hydrogen bond between His[57] and Asp[102] in serine proteinases (Robillard & Shulman, 1974). Similar signals were observed also in NMR spectra of the zymogens of wild-type and D189S rat trypsin (data not shown). Discontinuous histidine titration curves of the kind seen here were observed earlier for His[57] of porcine trypsin (Markley & Porubcan, 1976) and bovine and porcine trypsinogens (Porubcan et al., 1978) but not for other serine proteinases studied [reviewed in Markley (1978)]. Because of possible complications from autolysis, wild-type rat trypsin was not studied above pH 7. However, in the pH range investigated, the signals assigned to His[57] of wild-type rat trypsin were similar to those of the stable mutant D189S [see also Hedstrom et al. (1994)]. Modification of the residue at the base of the specificity pocket, thus, has no apparent effect on the properties of the catalytic histidine. This result validates the assumption made at the outset of these studies that the D189S mutant, which is much more stable than wild-type rat trypsin against autolysis, can serve as a valid model for studies of the catalytic region of the molecule.

The data of Figure 1 show that proton addition and loss to His[57] of both trypsin and its D189S mutant are slow on the NMR time scale. The peak at lower field corresponds to the protonated imidazole whereas that at higher field corresponds to the deprotonated imidazole. The pK_a' value can be estimated from the pH at which the areas of the two peaks are equivalent. The same analysis holds for the two complexes with α_1-PI. For the two free trypsin variants, this equivalence point is at about pH 7.0, whereas for the two complexes it is near pH 8.0. Thus it appears that the pK_a' values of His[57] of rat trypsin and its D189S mutant are higher by about one pH unit in the α_1-PI complexes (pK_a' about 8) than in the free proteinases (pK_a' about 7). The

spectra indicate, furthermore, that the Asp[102]−His[57] hydrogen bond is intact in these complexes, despite the formation of the assumed acyl linkage between the inhibitor and the enzyme. (If His[57] was not hydrogen bonded, the signal likely would be averaged with that from water.) The characteristic of the His[57] $H^{\delta 1}$ peak in both complexes are unusual, when compared to those observed (Markley, 1979) for serine proteinase-protein proteinase inhibitor complexes of the Michaelis-type (Baillargeon et al., 1977) such as trypsin-STI and trypsin-BPTI. The latter complexes show a relatively sharp His[57] $H^{\delta 1}$ peak with little temperature dependence of the line width and with no pH dependent chemical shift or intensity changes in the pH range studied here (Markley, 1979). By contrast, the corresponding peak in the α_1-PI−trypsin complexes is rather broad, shows a pH dependent chemical shift, and is resolved only moderately well at the low temperature at which data were collected (5 °C). This result indicates that the Asp[102]−His[57] diad is protected less well in the serpin complexes than in the Michaelis-type inhibitor complexes.

What may be additionally significant is that the pK_a' value for His[57], inferred from the pH dependence of the spectra, is higher in the α_1-PI complexes than in free rat trypsin. The increase in the pK_a' value of His[57] could contribute in a small way to the enhanced lifetime of the acyl-enzyme adduct. In a functional acyl-enzyme intermediate, the $N^{\epsilon 2}$ of His[57] is thought to be deprotonated and exposed to solvent so that it can accept a proton from the water molecule that attacks the acyl carbonyl. If, as the NMR data suggest, His[57] is more protonated in the complex than in the free enzyme at physiological pH, its catalytic activity as a general base would be reduced correspondingly.

The analogous signal from the hydrogen bond between His[57] and Asp[102] of α-chymotrypsin when complexed to recombinant human α_1-antichymotrypsin was not resolved in a previous NMR investigation (Plotnick et al., 1996). Although the authors interpreted this result to indicate that the His[57]−Asp[102] hydrogen bond is disrupted in this complex, the peak may simply have not been observed because the NMR data were collected at room temperature where the exchange of this hydrogen with solvent water may have broadened the signal beyond detection. It should be of interest to collect NMR data for the chymotrypsin−α_1-antichymotrypsin complex under the conditions used in the present study.

Additional Lines of Evidence for a Structural Change in Trypsin Accompanying Complex Formation. Several other experiments were carried out in order to further define the changes that occur in trypsin upon formation of the stable complex with α_1-PI. These studies revealed that, although trypsin in the complex is stabilized against thermal unfolding (Figures 4C,D and 5), it is destabilized against chemical denaturation (Figure 3C,D). Furthermore, trypsin in the complex becomes more susceptible to proteolysis by added trypsin (Kaslik et al., 1995) and to disulfide bond reduction by added DTT (Figure 7), and the trypsin−α_1-PI complex has a much higher affinity for ANS (Figure 6 and Table 1) most likely due to the deformed structure of trypsin. This result is reinforced by reports of increased ANS binding affinity for two other serpin−serine proteinase complexes: thrombin−ATIII (Atha et al., 1984) and C1s−C1 inhibitor (Lennick et al., 1985).

Since molten globule states of proteins (Ptitsyn, 1995) share the properties of enhanced susceptibility to limited proteolysis and disulfide bond reduction and increased ANS binding affinity, it is fair to ask whether binding to serpin causes a conformational transition in the proteinase from a native to a molten globule-like state. The results of the unfolding experiments, however, show that this is probably not the case. Properties of a true molten globule state include substantial loss of signal intensity in the near UV CD and the loss of a cooperative heat absorption peak in DSC (Ptitsyn, 1995). The trypsin D189S−α_1-PI complex retains its ordered structure in the vicinity of aromatic chromophores, as shown by the temperature dependence of the molar ellipticity at 282 nm (Figure 5B). In addition, the heat absorption peak of the complexed proteinase (T_m = 79 °C) is very similar to that of the uncomplexed enzyme (T_m = 72 °C), indicating a cooperative transition in both cases (Figure 4C,D). These results demonstrate that, in spite of its less-ordered structure, trypsin D189S in its complex with α_1-PI is native-like rather than molten globule-like.

Analysis of the results of the thermal and urea unfolding experiments reveals an interesting property of the trypsin D189S−α_1-PI complex. As judged from the near-UV CD, the tertiary structure of the complexed enzyme is disrupted (Figure 5B) at a temperature (about 79 °C) where the heat absorption maximum occurs in DSC (Figure 4), but from the far-UV CD data, it appears that the transition has little effect on the secondary structure (Figure 5A). Moreover, the urea-induced transition of the complexed enzyme affects only its tertiary structure. The far-UV CD spectra of the complex at 0 and 7 M urea are almost identical (data not shown), whereas the near-UV CD spectra (data not shown) and tryptophan emission spectra (Figure 3D) show that the tertiary structure of complexed enzyme is disrupted at 7 M urea. Thus, it is reasonable to suppose that both urea- and heat-induced structural transitions convert trypsin D189S complexed with α_1-PI into a molten globule-like state. This suggestion would explain why the urea-induced transition detected by tryptophan fluorescence (Figure 3D) is not visible in urea gradient gel (Figure 2D): the hydrodynamic volume of the molten globule form of a protein is much closer to that of the native form than that of the fully unfolded form (Ptitsyn, 1995); thus, the native → molten globule transition of the proteinase in the much larger complex may not lead to a detectable increase in the hydrodynamic volume as detected by the mobility of the complex on a urea gradient gel.

We conclude that four different structures of trypsin D189S can be differentiated in our experiments: the native, folded, uncomplexed enzyme (N); the native-like, but less-ordered complexed enzyme (S_1); the heat- and urea-induced, molten globule-like state (S_2); and the unfolded state (U). Interestingly, the native-like, but partially disordered structure of complexed trypsin mutant (S_1) is stabilized significantly (by 7 °C) against thermal unfolding (Figure 4). These results are similar to findings of no detectable thermal transitions for thrombin in ATIII (Atha et al., 1984) and for C1s in C1 inhibitor (Lennick et al., 1985) complexes, although the isolated components of the complexes undergo melting transitions, so the complexed thrombin and C1s seem to be more heat stable than their free forms. Surprisingly, however, trypsin in the complex was not stabilized against urea denaturation (Figure 3C,D). On the contrary, the

proteinase in the complex unfolds at a slightly lower urea concentration (5.8 M) than in the uncomplexed form (6.2 M). This finding is in agreement with the decreased stability of elastase when complexed with α_1-PI against GdnHCl induced unfolding (Hervé & Ghélis, 1991). The differential stability of the proteinase in the complex to thermal and chemical denaturants is unusual, and one may speculate that the less-ordered, more open structure of the complexed enzyme decreases its stability against chemical denaturants, whereas the extended interactions between the inhibitor and the proteinase play a role in the thermostability of the complex.

The results of the present unfolding experiments support the previous observation that the active site cleaved, RSL inserted serpins have a dramatically increased structural stability (Gettins & Harten, 1988; Bruch et al., 1988; Carell & Owen, 1985; Carell et al., 1991; Haris et al., 1990). Furthermore, the unfolding behavior of complexed α_1-PI was found to be very similar to that of α_1-PI*: no unfolding transition was observed for either, even in 8 M urea (Figure 2B,D; Figure 3B,D), and thermal unfolding of both forms was around 124 °C (Figure 4B,D). This observation suggests that the conformation of α_1-PI in the trypsin−proteinase inhibitor complex is similar to that of its cleaved α_1-PI* form [see Shore et al. (1995), Lawrence et al. (1995), Plotnick et al. (1996), Mast et al. (1991), Björk et al. (1993), Olson et al. (1995), and Debrock and Declerck (1995)].

Current Understanding of the Structure of the Complex. The P1-P1′ site of the inhibitor is cleaved in the complex, and the proteinase and serpin are linked covalently by an acyl bridge between the O^{γ} of the catalytic Ser^{195} (on the border of the activation domain) of the proteinase and the C′ of Met^{358} of the serpin (Shore et al., 1995; Kaslik et al., 1995; Lawrence et al., 1995; Wilczynska et al., 1995; Engh et al., 1995). The present results, along with those from limited proteolysis (Kaslik et al., 1995; Stavridi et al., 1996), indicate that complex formation stabilizes the overall structure of the proteinase but leads to a conformational change that appears to disorder a limited part of the structure. This conformational change does not disrupt the hydrogen bond between His^{57} and Asp^{102}, but it does raise the pK_a' of His^{57} by about one pH unit.

The trypsin family of serine proteinases undergo a well-known conformational transition that involves disorder−order of the region adjacent to Ser^{195}: the conversion between the zymogen and activated enzyme states (Huber & Bode 1978). The inactive precursor proenzyme, or zymogen form of trypsin-like serine proteinases can be termed as a folding intermediate for the active, properly folded enzyme, and the parts of the molecule, which are involved in the structural rearrangement of activation process are thought to be a late folding unit, called "activation domain" (residues in trypsin: 16−19, 142−152, 184−194, and 216−224) (Huber & Bode 1978). The activation domain is less ordered, more flexible in trypsinogen than in the activated proteinase. Furthermore, a recent proposal suggests that the mechanism of serine proteinase action may involve structural movements of some parts of the activation domain (Gráf, 1995).

It is tempting to speculate that a conformational change in the plastic activation domain of the trypsin structure, especially in one of the loops (residues 184−194) also accompanies formation of the trypsin−α_1-PI complex. This notion is reinforced by the finding that the pK_a' of His^{57} in the complex resembles that in the zymogen. The increased binding affinity of ANS to the trypsin D189S−α_1-PI complex (Figure 6) and the apparent lability of the disulfide bond network in the complexed proteinase (Figure 7) are also consistent with this view. As to the latter property, a disulfide bond between two loops of the activation domain (Cys^{191}−Cys^{220}) may be the "weakest point" of the deformed network of disulfide bridges in the complex, in analogy to the increased accessibility of this bond in trypsinogen as compared to trypsin (Light et al., 1969). Additionally, Stavridi et al. (1996) have recently proposed that formation of the α-chymotrypsin−α_1-antichymotrypsin complex involves displacement or destabilization of the Ile^{16}−Gly^{25} segment of α-chymotrypsin in order to explain the exposure of sites cleaved by HNE (Val^{188}, Ala^{158}, and Thr^{139}). Both the Ile^{16}−Gly^{25} segment and the cleavage sites are very close or even belong to the activation domain. It is worth noting here that the bacterial serine proteinase subtilisin, which has no activation domain-like structural element owing to its different mechanism of activation, is inactivated only temporarily by α_1-PI; subtilisin treats α_1-PI as a substrate rather than as an inhibitor (Abe & Kuromizu, 1989). Thus, we conclude that the plastic activation domain of trypsin-like serine−proteinase structures may play a crucial role in the inhibitor-induced structural rearrangement of the proteinase.

In summary, we suggest that the process of complex formation with α_1-PI converts trypsin D189S into an inactive, loose structure, which serves as a "conformational trap" of the enzyme that prevents catalytic deacylation. We believe that this trap mechanism could be general for inhibitory serpins and that it may facilitate the degradation and removal of the target proteinases *in vivo*.

REFERENCES

Abe, O., & Kuromizu, K. (1989) *J. Biochem. 105*, 66−71.

Aertgeerts, K., De-Bondt, H. L., De-Ranter, C., & Declerck, P. J. (1995) *Proteins 23*, 118−121.

Atha, D. H., Brew, S. A., & Ingham, K. C. (1984) *Biochim. Biophys. Acta 785*, 1−6.

Baillargeon, M. W., Laskowski, M., Jr., Neves, D. E., Porubcan, M. A., Santini, R. E., & Markley, J. L. (1980) *Biochemistry 19*, 5703−5710.

Baumann, U., Huber, R., Bode, W., Grosse, D., Lesjak, M., & Laurell, C. B. (1991) *J. Mol. Biol. 218*, 595−606.

Baumann, U., Bode, W., Huber, R., Travis, J., & Potempa, J. (1992) *J. Mol. Biol. 226*, 1207−1218.

Björk, I., Nordling, K., & Olson, S. T. (1993) *Biochemistry 32*, 6501−6505.

Bruch, M., Weiss, V., & Engel, J. (1988) *J. Biol. Chem. 263*, 16626−16630.

Carell, R. W., & Owen, M. C. (1985) *Nature 317*, 730−732.

Carell, R. W., Evans, D. L., & Stein, P. E. (1991) *Nature 353*, 576−578.

Christensen, S., Valnickova, Z., Thøgersen, I. B., Pizzo, S. V., Nielsen, H. R., Roepstorff, P., & Enghild, J. J. (1995) *J. Biol. Chem. 270*, 14859−14862.

Cohen, A. B., Geczy, D., & James, H. L. (1978) *Biochemistry 17*, 392−400.

Corey, D. R., & Craik, C. S. (1992) *J. Am. Chem. Soc. 114*, 1784−1790.

Creighton, T. E. (1979) *J. Mol. Biol. 129*, 235−264.

Debrock, S., & Declerck, P. J. (1995) *FEBS Lett 376*, 243−246.

Elliott, P. R., Lomas, D. A., Carrell, R. W., & Abrahams, J. P. (1996) *Nat. Struct. Biol. 3*, 676−681.

Engh, R., Huber, R., Bode, W., & Schulze, A. J. (1995) *Trends Biotechnol. 13*, 503−510.

Enghild, J. J., Valnickova, Z., Thøgersen, I. B., & Pizzo, S. V. (1994) *J. Biol. Chem. 269*, 20159−20166.
Gettins, P., & Harten, B. (1988) *Biochemistry 27*, 3634−3639.
Goldenberg, D. P. (1989) *Protein structure: A practical approach* (Creighton, T. E., Ed.) pp 225−250, IRL Press, New York.
Gráf, L. (1995) in *Natural sciences and human thought* (Zwilling, R., Ed.) pp 139−148, Springer-Verlag, Berlin.
Gráf, L., Jancsó, A., Szilágyi, L., Hegyi, G., Pintér, K., Náray-Szabó, G., Hepp, J., Medzihradszky, K., & Rutter, W. J. (1988) *Proc. Natl. Acad. Sci. U.S.A. 85*, 4961−4965.
Haris, P. I., Chapman, D., Harrison, R. A., Smith, K. F., & Perkins, S. J. (1990) *Biochemistry 29*, 1377−1380.
Hedstrom, L., Farr-Jones, S., Kettner, C. A., & Rutter, W. J. (1994) *Biochemistry 33*, 8764−8769.
Hervé, M., & Ghélis, C. (1991) *Arch. Biochem. Biophys. 285*, 142−146.
Hore, P. J. (1983) *J. Magn. Reson. 55*, 283−300.
Huber, R., & Bode, W. (1978) *Acc. Chem. Res. 11*, 14−122.
Johnson, D. A., & Travis, J. (1976) *Biochem. Biophys. Res. Commun. 72*, 33−39.
Kaslik, G., Patthy, A., Bálint, M., & Gráf, L. (1995) *FEBS Lett. 370*, 179−183.
Komiyama, T., Ray, C. A., Pickup, D. J., Howard, A. D., Thornberry, N. A., Peterson, E. P., & Salvesen, G. (1994) *J. Biol. Chem. 29*, 19331−19337.
Laemmli, U. K. (1970) *Nature 227*, 680−685.
Lawrence, D. A., Ginsburg, D., Day, D. E., Berkenpas, M. B., Verhamme, I. M., Kvassman, J. O., & Shore, J. D. (1995) *J. Biol. Chem. 270*, 25309−25312.
Lennick, M., Brew, S. A., & Ingham, K. C. (1985) *Biochemistry 24*, 2561−2568.
Light, A., Hardwick, B. C., Hatfield, L. M., & Sondack, D. L. (1969) *J. Biol. Chem. 244*, 6289−6296.
Lindahl, T. L., Ohlsson, P. I., & Wiman, B. (1990) *Biochem. J. 265*, 109−113.
Löbermann, H., Tokuoka, R., Deisenhofer, J., & Huber, R. (1984) *J. Mol. Biol. 177*, 531−556.
Markley, J. L. (1978) *Biochemistry 17*, 4648−4656.
Markley, J. L. (1979) in *Magnetic resonance studies in biology* (Shulman, R. G., Ed.) pp 397−461, Academic Press, New York.
Markley, J. L., & Porubcan, M. P. (1976) *J. Mol. Biol. 102*, 487−509.
Mast, A. E., Enghild, J. J., Pizzo, S. V., & Salvesen, G. (1991) *Biochemistry 30*, 1723−1730.
Matheson, N. R., van Halbeek, H., & Travis, J. (1991) *J. Biol. Chem. 266*, 13489−13491.
Moroi, M., & Yamasaki, M. (1974) *Biochim. Biophys. Acta. 359*, 130−141.
Mourey, L., Samama, J.-P., Delaure, M., Petitou, M., Choay, J., & Moras, D. (1993) *J. Mol. Biol. 232*, 223−241.
Nilsson, T., Sjöholm, I., & Wiman, B. (1983) *Biochem. J. 213*, 617−624.
Olson, S. T., Bock, P. E., Kvassman, J., Shore, J. D., Lawrence, D. A., Ginsburg, D., & Björk, I. (1995) *J. Biol. Chem. 270*, 30007−30017.
Owen, W. G. (1975) *Biochim. Biophys. Acta 405*, 380−387.
Plotnick, M. I., Mayne, L., Schechter, N. M., & Rubin, H. (1996) *Biochemistry 35*, 7586−7590.
Porubcan, M. A., Neves, D. E., Rausch, S. K., & Markley, J. L. (1978) *Biochemistry 17*, 4640−4647.
Privalov, P. L. (1979) *Adv. Protein Chem. 33*, 167−241.
Ptitsyn, O. B. (1995) *Adv. Protein Chem. 47*, 83−229.
Robillard, G., & Shulman, R. G. (1974) *J. Mol. Biol. 86*, 519−540.
Schechter, I., & Berger, A. (1967) *Biochem. Biophys. Res. Commun. 27*, 157−162.
Shieh, B.-H., Potempa, J., & Travis, J. (1989) *J. Biol. Chem. 264*, 13420−13423.
Shore, J. D., Day, D. E., Francis-Chmura, A. M., Verhamne, I., Kvassman, J., Lawrence, D. A., & Ginsburg, D. (1995) *J. Biol. Chem. 270*, 5395−5398.
Song, H. K., Lee, K. N., Kwon, K. S., Yu, M. H., & Suh, S. W. (1995) *FEBS Lett. 377*, 150−154.
Stavridi, E. S., O'Malley, K., Lukacs, C. M., Moore, W. T., Lambris, J. D., Christianson, D. W., Rubin, H., & Cooperman, B. S. (1996) *Biochemistry 35*, 10608−10615.
Stryer, L. (1965) *J. Mol. Biol. 13*, 482−495.
Wei, A., Rubin, H., Cooperman, B. S., & Christianson, D. W. (1994) *Nat. Struct. Biol. 1*, 251−258.
Wilczynska, M., Fa, M., Ohlsson, P. I., & Ny, T. (1995) *J. Biol. Chem. 270*, 29652−29655.
Wiman, B., & Collen, D. (1979) *J. Biol. Chem. 254*, 9291−9297.

BI962931M